Available online at www.sciencedirect.com
ScienceDirect
Journal of Sound and Vibration 311 (2008) 1286–1304
JOURNAL OF SOUND AND VIBRATION
www.elsevier.com/locate/jsvi

A method for analyzing absorbed power distribution in the hand and arm substructures when operating vibrating tools

Jennie H. Dong[a], Ren G. Dong[b,*], Subhash Rakheja[a], Daniel E. Welcome[b], Thomas W. McDowell[b], John Z. Wu[b]

[a]*Department of Mechanical Engineering, CONCAVE Research Centre, Concordia University, 1455 de Maisonneuve Blvd. West, Montreal, Canada*
[b]*Engineering & Control Technology Branch, National Institute for Occupational Safety and Health, 1095 Willowdale Road, MS L-2027, Morgantown, WV 26505, USA*

Received 30 January 2007; received in revised form 22 August 2007; accepted 10 October 2007
Available online 26 November 2007

Abstract

In this study it was hypothesized that the vibration-induced injuries or disorders in a substructure of human hand–arm system are primarily associated with the vibration power absorption distributed in that substructure. As the first step to test this hypothesis, the major objective of this study is to develop a method for analyzing the vibration power flow and the distribution of vibration power absorptions in the major substructures (fingers, palm–hand–wrist, forearm and upper arm, and shoulder) of the system exposed to hand-transmitted vibration. A five-degrees-of-freedom model of the system incorporating finger- as well as palm-side driving points was applied for the analysis. The mechanical impedance data measured at the two driving points under four different hand actions involving 50 N grip-only, 15 N grip and 35 N push, 30 N grip and 45 N push, and 50 N grip and 50 N push, were used to identify the model parameters. The vibration power absorption distributed in the substructures were evaluated using vibration spectra measured on many tools. The frequency weightings of the distributed vibration power absorptions were derived and compared with the weighting defined in ISO 5349-1 (2001). This study found that vibration power absorption is primarily distributed in the arm and shoulder when operating low-frequency tools such as rammers, while a high concentration of vibration power absorption in the fingers and hand is observed when operating high-frequency tools, such as grinders. The vibration power absorption distributed in palm–wrist and arm is well correlated with the ISO-weighted acceleration, while the finger vibration power absorption is highly correlated with unweighted acceleration. The finger vibration power absorption-based frequency weighting suggested that exposure to vibration in the frequency range of 16–500 Hz could pose higher risks of developing finger disorders. The results support the use of the frequency weighting specified in the current standard for assessing risks of developing disorders in the palm–wrist–arm substructures. The standardized weighting, however, could overestimate low-frequency effects but greatly underestimate high-frequency effects on the development of finger disorders. The results are further discussed to show that the trends observed in the vibration power absorptions distributed in the substructures are consistent with some major findings of various physiological and epidemiological studies, which provides a support to the hypothesis of this study.

*Corresponding author. Tel.: +1 304 285 6332; fax: +1 304 285 6265.
E-mail address: rkd6@cdc.gov (R.G. Dong).

0022-460X/$ - see front matter © 2007 Elsevier Ltd. All rights reserved.
doi:10.1016/j.jsv.2007.10.031

1. Introduction

Vibration exposure could be a source of annoyance or discomfort. More critically, epidemiological studies have confirmed that prolonged intensive exposure to hand-transmitted vibration can potentially cause a series of disorders in the vascular, sensorineural and musculoskeletal structures of the human hand–arm system [1], which have been collectively termed as hand–arm vibration syndrome [2]. The severity and locations of localized discomforts and/or disorders usually depend on the types of tools used by the operator, since different tools transmit vibrations that are not only significantly different in magnitudes but also in frequencies. Although many studies on exposure and health effects have been reported and an international standard on the measurement, evaluation and risk assessment of exposure has been established [3], a reliable dose–response relation for any component of hand–arm vibration syndrome has not yet been developed [4]. In order to develop a better relationship, further systematic efforts are highly desirable not only on the health effects but also on the formulation of the exposure dosage.

Knowledge of the complex biodynamic responses of fingers, hand and arm can be used to help interpret the phenomena observed in reported epidemiological and physiological studies on hand–arm vibration syndrome [5–7]. Characterizing frequency-dependent biodynamic responses can also help define a new frequency weighting for hand–arm vibration syndrome and for other upper limb disorders associated with exposure to hand-transmitted vibration and thereby more reliable dose–response relationships (see, for example, Ref. [8]). Vibration power absorption into the hand–arm system is one of the most important biodynamic measures that can be used to quantify the vibration exposure for assessing its potential effects. Although the exact relationship between the amount of absorbed power and the cell or tissue damage remains unknown, the vibration power absorption can be simply regarded as a physical measure of vibration-induced mechanical stimulus that acts directly on the cells and tissues [6,7]. The vibration power absorption can take into account not only the vibration hazard measured on a tool but also the physical response of the hand–arm system. The effects of some of the influencing factors, such as hand and arm postures, applied hand forces, and tool handle sizes, can also be automatically reflected in such a measure [9,10]. Therefore, the use of vibration power absorption of the entire hand–arm system has been advocated to assess the risk of the most common hand–arm vibration syndrome component: vibration-induced white finger [11]. It has also been suggested that the total vibration power absorption could yield a better estimate of exposure than the ISO frequency-weighted acceleration for risk assessment of hand-transmitted vibration [11,12].

Whereas the general hypothesis of the power absorption approach seems reasonable, the total energy method has been questioned [8,13]. A few researchers have recently reported that the frequency weighting derived from the total vibration power absorption is highly consistent with the ISO frequency weighting [3] established mainly on the basis of subjective sensation data reported by Miwa [14,15]. These observations suggest that the total energy method perhaps offers a potential for assessing the overall discomfort but it would not be likely to provide a better prediction of vibration-induced white finger than the current ISO method [8].

The major deficiency of the total energy method is that it ignores the distribution of power absorption in the hand–arm system, and the power flow and concentration effects [13]. Alternatively, determination of localized vibration power absorption or its distribution and its frequency dependency could help overcome this deficiency. Although many other factors such as finger temperature and vibration-induced global physiological and pathological responses (e.g., center nerve reaction and blood flow reduction in the hand–arm system) could influence the development of vibration-induced white finger, it is worthwhile to test the hypothesis that the power absorption related to most damage is that which is largely distributed in the fingers because the symptoms of vibration-induced white finger are localized in this area [16]. Similarly, it is also reasonable to hypothesize that the vibration-induced disorders in the wrist are mainly related to power absorbed within the palm, wrist, and forearm substructures.

In order to test this local energy method, it is necessary to quantify vibration power absorption in the various substructures of the hand–arm system, namely fingers, palm–hand–wrist, arms, and shoulder. Whereas the vibration power absorption of the entire hand–arm system can be reliably measured at the hand–handle interface using an instrumented handle, a feasible technique has not been developed to directly measure the vibration power absorption distributed in any of the substructures. Although the biodynamic

response of a fingertip can be predicted using a finite element model [17], analyses of power distributed in entire hand–arm system using the finite element technique remains a formidable task. A methodology to separately measure the flow of vibration power into the fingers and the palm of hand has been proposed [13]. The power measured at the fingers or the palm, however, may not be fully absorbed in the fingers or the palm and it may further flow into remaining substructures of the hand–arm system. Clearly, an alternate method for quantifying the amount of power absorbed in specific substructures is highly desirable.

This study primarily aims at developing a modeling approach to predict the vibration power absorption in major substructures of the hand–arm system. A new mechanical-equivalent model of the hand–arm system was developed on the basis of mechanical impedance measured at the fingers and the palm under exposure to vibration along the forearm direction (z_h-axis). The model was analyzed to derive distributed vibration power absorptions and their frequency weightings, which were compared with the weighting specified in ISO 5349-1 [3]. As examples, the distributed vibration power absorptions of many powered hand tools were also predicted and used to analyze the correlations among the acceleration and vibration power absorption measures. Attempts were also made to explore the interpretations of the distributed vibration power absorptions in view of those deduced from reported epidemiological and physiological studies.

2. Methods

2.1. Model of the hand–arm system

Fig. 1 shows the structure of the hand–arm system model recently proposed by a few researchers [18]. Different from the reported models that invariably assume a single-point hand–handle coupling relationship [19,20], this model assumes a two-point coupling between the hand and the handle. The hand gripping a vibrating handle is represented by a clamp-like mechanical system by dividing the hand into two major parts about the centerline of a cylindrical handle. The first part constitutes the fingers positioned on one side of the handle, and represented by two masses (M_4 and M_2) coupled through linear stiffness (k_4) and viscous damping (c_4). Mass M_4 represents the effective mass of fingers' skin contacting the handle. Mass M_2 is the effective mass due to the remaining finger tissues, mainly composed of mass of fingers' bones. The power absorbed within the fingers can be derived from the energy dissipated by c_4, which is directly related to relative movement between the two masses (M_2 and M_4). The power absorbed within the fingers is thus referred to as c_4-vibration power absorption.

As also shown in Fig. 1, the second part comprises the palm–wrist–forearm substructure and is represented by two masses (M_3 and M_1) coupled through k_3 and c_3. Whereas M_3 represents the effective mass of palm skin

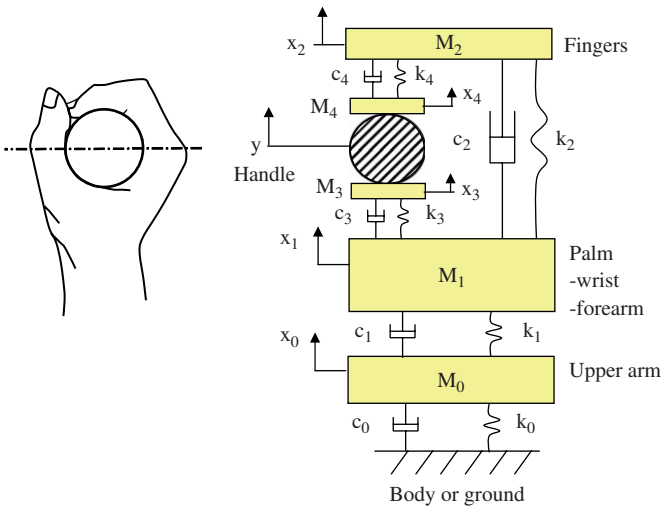

Fig. 1. Handgrip posture and the configuration of a five-degree-of-freedom model of the hand–arm system.

contacting the handle and M_1 is effective mass of palm–wrist–forearm substructure. The energy dissipated by c_3 directly relates to relative motion between the forearm bones and the palm–handle contact surface, and can thus be used to represent vibration power absorption in the palm, wrist, and part of the forearm tissues (c_3-vibration power absorption). The major equivalent mass of the fingers (M_2) and the major equivalent mass of the palm–wrist–forearm (M_1) are coupled through linear spring-damping elements (k_2 and c_2) coupling. The dissipated energy by c_2, derived from relative motion between the two substructures, is mostly attributed to rotational motions of the hand's metacarpo-phalangeal joints. The c_2-vibration power absorption can be interpreted as the vibration power absorption distributed in the hand back, and the metacarpo-phalangeal joints and their surrounding tissues.

The effective palm–wrist–forearm mass M_1 is connected to the effective mass of the upper arm–shoulder structure (M_0) through another spring-damping element (k_1 and c_1). The c_1-vibration power absorption can be used to represent the power absorbed by the tissues in the forearm, upper arm, and part of the shoulder. Mass M_0 is coupled to fixed ground through another spring-damping element (k_0, and c_0). The c_0-vibration power absorption is thus considered to represent the power absorbed in the shoulder and that transmitted beyond the shoulder and absorbed in other parts of the body such as neck and head.

Results of a few studies suggest that the biodynamic response of the human hand–arm system to hand-transmitted vibration is non-linear [17,21]. The hand forces (grip and push) particularly influence the vibration power absorption in a nonlinear manner. In this study, the non-linear behaviors are considered by identifying model parameters as functions of applied hand forces using the measured data acquired under various combinations of hand forces. A linear model corresponding to a particular hand force, however, is assumed.

The equations of motions of the five-degrees-of freedom linear model subject to handle excitation $y(t)$ are expressed in the matrix form as

$$[M]\{\ddot{q}\} + [C]\{\dot{q}\} + [K]\{q\} = \{F\}, \tag{1}$$

where $[M]$ is mass matrix, $[C]$ is damping matrix, $[K]$ is stiffness matrix, $\{F\}$ is forcing vector and $\{q\}$ is vector response coordinates.

The equations of motion can be solved by assuming $y = Ye^{j\omega t}$, and the biodynamic forces acting at the fingers–handle and palm–handle interfaces can be calculated from the system responses and given parameters. Then, the driving-point mechanical impedances distributed at the fingers (Z_{Fingers}) and the palm (Z_{Palm}) can be calculated from

$$Z_{\text{Fingers}}(j\omega) = \frac{(k_4 + j\omega c_4)(Y - X_2)}{j\omega Y} + M_4 j\omega = Z_{\text{Fingers\_Re}} + jZ_{\text{Fingers\_Im}}, \tag{2}$$

$$Z_{\text{Palm}}(j\omega) = \frac{(k_3 + j\omega c_3)(Y - X_1)}{j\omega Y} + M_3 j\omega = Z_{\text{Palm\_Re}} + jZ_{\text{Palm\_Im}}, \tag{3}$$

where Y is magnitude of handle excitation displacement, X_1 and X_2 are displacement magnitudes of masses M_1 and M_2, respectively, $j = \sqrt{-1}$ and ω is excitation frequency.

2.2. Experimental data for model construction

A total of 15 parameters are identified for the model using the experimental data reported in two studies [22,23]. Briefly, ten subjects participated in experiments for measuring the biodynamic responses distributed at both the fingers and the palm of the hand under a broadband random vibration excitation along z_h-axis in the 10–1000 Hz range. Each subject was instructed to stand upright on a force plate for push force measurement and to hold an instrumented handle, as shown in Fig. 2, for the grip force and biodynamic force measurements. The elbow angle was controlled at approximately $90 \pm 10^\circ$, without touching the body during the measurements. The measured biodynamic force and acceleration data were analyzed to derive finger and palm-side mechanical impedances, expressed in the one-third octave band frequencies from 10 to 1000 Hz. Four test treatments involving different hand forces (50 N grip-only, 15 N grip and 35 N push, 30 N grip and 45 N push, 50 N grip and 50 N push) were considered in measurements of finger- as well as palm-side responses. The biodynamic response of the entire hand–arm system was derived from summation of responses at the fingers and the palm [13].

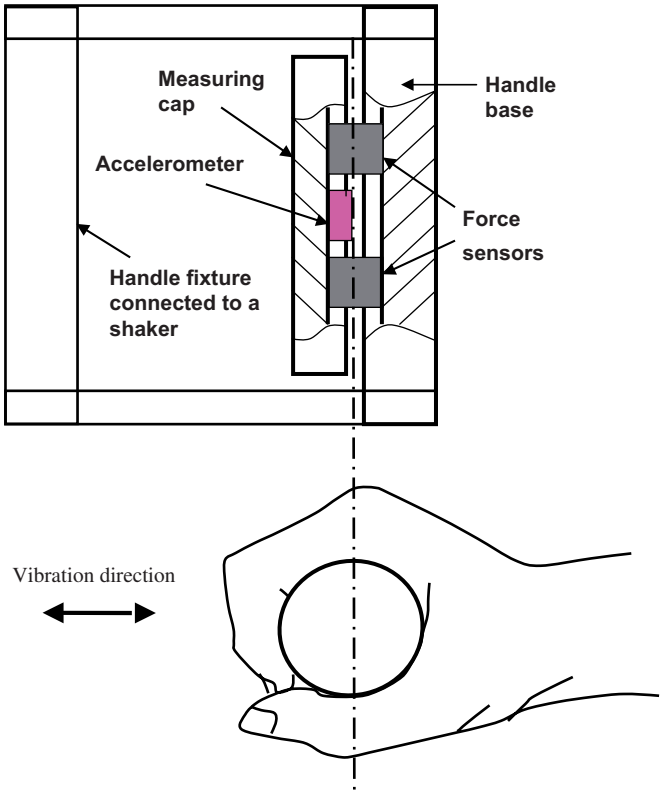

Fig. 2. The instrumented handle (40 mm in diameter and 115 mm effective grip length) used for measuring the mechanical impedances distributed at the fingers and the palm of the hand [22,23].

2.3. Determination of model parameters

The model parameters were identified using the measured data through solution of a constrained error minimization problem, where the error function was formulated as the deviation between the measured and model impedance responses [18]. The available anthropometry data for the human hand–arm system [24,25] are used to identify limits of the model masses, which are expressed by the following inequality constraints:

$$
\begin{aligned}
&M_0, M_1, M_2, M_3, M_4, k_0, k_1, k_2, k_3, k_4, c_0, c_1, c_2, c_3, c_4 > 0,\\
&M_0 < 15\,\text{kg (shoulder and a part of upper body)},\\
&M_1 < 5\,\text{kg (palm, hand back, wrist, and forearm)},\\
&M_2 < 200\,\text{g (fingers bones and part of the finger soft tissues)},\\
&M_3 < 50\,\text{g (palm contact skin)},\\
&M_4 < 30\,\text{g (finger contact skin)}.
\end{aligned} \tag{4}
$$

The above constraints together with the parameter values obtained from a previous modeling study [18] were used to identify the initial parameter vector. The fingers- and palm-side driving-point mechanical impedances were computed using Eqs. (1)–(3) and the initial model parameters. The deviation (ΔZ) between the measured and model impedance values were then computed from

$$
\Delta Z = \sqrt{\frac{1}{N}\sum_{i=1}^{N}(Z_{P_i} - Z_{E_i})^2}, \tag{5}
$$

where Z_{P_i} and Z_{E_i} are predicted and experimental impedance values measured at the fingers or the palm at center frequency of the ith frequency band, respectively, and N is the number of one-third octave frequency bands considered in the analysis. An error function $E(\chi)$, comprising the sum of deviations in Z_{Fingers} and Z_{Palm}, is formulated as

$$E(\chi) = \text{Re}[\Delta Z_{\text{Fingers}}(\text{j}\omega)] + \text{Im}[\Delta Z_{\text{Fingers}}(\text{j}\omega)] + \text{Re}[\Delta Z_{\text{Palm}}(\text{j}\omega)] + \text{Im}[\Delta Z_{\text{Palm}}(\text{j}\omega)], \tag{6}$$

where 'Re' and 'Im' designate the real and imaginary components of impedance, respectively, corresponding to center frequency ω; and χ is the vector of model parameters, given by

$$\chi = [M_0, M_1, M_2, M_3, M_4, k_0, k_1, k_2, k_3, k_4, c_0, c_1, c_2, c_3, c_4].$$

For model parameter identification, each model parameter is varied sequentially until the resulting error function in Eq. (6) attains a minimum value. The process is repeated until the solutions corresponding to two consecutive iterations converge to similar error values. The process was considered to yield model parameters when the difference between impedance error values corresponding to two consecutive iterations was less than 0.01 Ns/m. The solutions were attained for different sets of the initial parameters that were randomly selected within the constraints defined in Eq. (4). The solutions converged to very similar values for each parameter (difference $<1\%$). The validity of the solutions was further verified using a perturbation method. Variations in the identified parameters in both increasing and decreasing direction resulting in relatively larger error values, suggesting the validity of the solutions around a local minimum.

2.4. Calculations of vibration power absorption

The model was analyzed to evaluate the driving point impedances, while the absorbed power transmitted to the fingers ($P_{\text{F\_Fingers}}$) and the palm ($P_{\text{F\_Palm}}$) were derived from the mechanical impedances as [8]

$$P_{\text{F\_Fingers}}(\omega) = \tfrac{1}{2}\text{Re}[Z_{\text{Fingers}}(\text{j}\omega)]|V_{\text{Handle}}(\text{j}\omega)|^2, \tag{7}$$

$$P_{\text{F\_Palm}}(\omega) = \tfrac{1}{2}\text{Re}[Z_{\text{Palm}}(\text{j}\omega)]|V_{\text{Handle}}(\text{j}\omega)|^2, \tag{8}$$

where V_{Handle} is handle vibration velocity.

The total power absorbed in the entire hand–arm system (P_{Total}) in the band centered at frequency ω can be computed from the sum of powers distributed in the fingers and the palm [13], such that

$$P_{\text{Total}}(\omega) = P_{\text{F\_Fingers}}(\omega) + P_{\text{F\_Palm}}(\omega). \tag{9}$$

The total power is absorbed in the damping elements of the hand–arm system model. In the specific model used in this study, the total power is dissipated by the five dampers, which can be expressed as

$$P_{\text{Total}}(\omega) = \sum_{k=1}^{5} P_k(\omega) = \frac{1}{2}\sum_{k=1}^{5} c_k[\Delta V_k(\omega)]^2, \tag{10}$$

where ΔV_k is amplitude of relative velocity across the viscous damping element k. As above-mentioned, the energy dissipated within individual dissipative elements can describe the distribution of vibration power absorption within various substructures of the hand–arm system.

The vibration measured on a tool is usually expressed as the root-mean-square acceleration (A_{Tool}) in the one-third octave band. The above relationships for the total power absorbed within the hand–arm system can also be expressed in terms of root-mean-square acceleration value, such that

$$P_{\text{Total}}(\omega) = \text{Re}[Z_{\text{Fingers}}(\text{j}\omega)]\left[\frac{A_{\text{Tool}}(\omega)}{\omega}\right]^2 + \text{Re}[Z_{\text{Palm}}(\text{j}\omega)]\left[\frac{A_{\text{Tool}}(\omega)}{\omega}\right]^2, \tag{11}$$

$$P_k(\omega) = c_k[\Delta V_{k\_\text{rms}}(\omega)]^2, \tag{12}$$

where ΔV_{k_rms} is the relative velocity across c_k, which is evaluated from the model subjected to root-mean-square acceleration excitation at the handle.

The total power absorbed in kth substructure in the entire frequency range of concern can be derived upon summation of the powers within individual bands, such that

$$\bar{P}_k = \sum_{i=1}^{n} P_k(\omega_i), \tag{13}$$

where $\bar{P}_k$ is total vibration power absorption of the kth substructure and n is number of one-third octave frequency bands.

With the vibration power absorption measure, the energy absorbed in the entire system or each substructure over an exposure period T can be used to derive the vibration exposure dose (E) of the corresponding system or substructure for the exposure period, which is expressed as

$$E_k = T \sum_{i=1}^{n} P_k(\omega_i). \tag{14}$$

This exposure dosage value based on vibration power absorption may be potentially used to examine the dose–response relationship between the vibration exposure and its health effects.

2.5. Frequency weighting of the vibration power absorption

Alternatively, the vibration power absorption measure can be expressed by an acceleration measure [8]. An acceleration-based exposure dose similar to that defined in ISO 5349-1 [3] can be derived to examine the dose–response relationship. The frequency weightings of the vibration power absorption with respect to acceleration due to vibration of a tool can be derived from Eqs. (11) and (12). Such frequency weightings can also be determined by assuming a constant acceleration at each center frequency of the one-third octave bands. The vibration power absorption measure (expressed in Watts), however, is physically different from the acceleration measure (m/s^2) and the vibration power is approximately proportional to square of acceleration magnitude. From Eqs. (11) and (12), it can be seen that the power obtained with constant acceleration spectrum cannot be directly used to represent the vibration power absorption weighting for comparison with the ISO weighting defined in ISO 5349-1 [3]. This issue can be resolved by taking the square root of the vibration power absorption and normalizing the resulted measure [8]. Therefore, the vibration power absorption-based frequency weighting that is directly comparable with the ISO weighting in the one-third octave bands is defined as follows:

$$W(\omega_i) = 0.958 \frac{\sqrt{P(\omega_i)}}{\sqrt{P_{\mathrm{Max}}}}, \quad i = 1, 2, \ldots, n, \tag{15}$$

where $W(\omega_i)$ is vibration power absorption weighting corresponding to center frequency ω_i in the one-third octave bands, the constant value 0.958 equals the peak magnitude of the weighting function defined in ISO-5349-1 (2001), and P_{Max} is the maximum value of the power absorption spectrum calculated using a constant acceleration at each center frequency of the one-third octave band.

2.6. Correlation analyses

Linear correlation analyses of different measures including vibration power absorption, acceleration and ISO-weighted acceleration, were performed using vibration spectra of different tools. The results were used to explore the sensitivity of differences among distributed vibration power absorptions, the ISO-weighted acceleration, and unweighted acceleration in a practical application, linear correlation analyses of these vibration measures were performed. The vibration spectra of 20 different tools, reported by Griffin [26], were used to compute all three vibration measures. The selected vibration spectra were considered to represent the transmitted vibration of a wide range of powered hand tools. The weighted root-mean-square acceleration due to each tool was computed from

$$A_m = \sqrt{\sum_{i=1}^{21} [W_m(\omega_i) A_{\mathrm{tool}}(\omega_i)]^2}, \tag{16}$$

where A_m is overall root-mean-square acceleration measure and W_m is weighting factor corresponding to m type of vibration measure. An unweighted root-mean-square acceleration measure is obtained by letting $W_m = 1$. The W_m may assume either vibration power absorption- or ISO-based weighting values. In this study, both the energy and acceleration measures were obtained over the 10–1000 Hz frequency range.

3. Results

3.1. Established models

The model parameters identified for the four sets of hand forces are summarized in Table 1. The table also lists the model natural frequencies (f_0, f_1, f_2) and damping ratios (ξ_0, ξ_1, ξ_2) that were derived from the eigenvalue analysis. It is interesting to note that the effective masses (M_3 and M_4) of skin in contact with vibrating handle and the finger mass (M_2) vary within narrow ranges over the ranges of hand forces considered. As expected, the fingers' contact stiffness and damping values (k_4, c_4) increase with increase in the fingers-applied force (grip force). The palm contact stiffness and damping values (k_3, c_3) also increase with the increase in the palm-applied force (combined grip and push force).

Fig. 3 illustrates comparisons of mechanical impedance magnitude and phase responses of the model with the corresponding experimental data measured at the fingers and the palm of the hand. The comparison of the predicted total/hand impedance and that summed from the finger and palm impedances is also illustrated in this figure. The results show very good agreement between the model and measured responses in the entire frequency range, irrespective of the hand forces considered. The lowest correlation coefficient obtained among all the comparisons was 0.96. These comparisons suggest that the model fits the experimental data very well in every case. The impedance curves shown in Fig. 3 suggest two major resonances (the vicinity of the peaks in the graph) of the hand–arm system, occurring in the 16–50 and 100–300 Hz ranges. The lower resonant frequency is close to that estimated from palm contact stiffness (k_3) and palm–wrist–forearm effective mass

Table 1
Model parameters

Parameter	Unit	Hand actions			
		50 N grip	15 N grip + 35 N push	30 N grip + 45 N push	50 N grip + 50 N push
M_0	kg	5.854	6.099	6.505	5.863
M_1	kg	1.324	0.850	0.977	1.248
M_2	kg	0.083	0.084	0.080	0.083
M_3	kg	0.025	0.029	0.031	0.029
M_4	kg	0.013	0.011	0.012	0.013
K_0	N/m	13,740	17,272	18,826	16,903
K_1	N/m	2462	2416	1018	1698
K_2	N/m	6788	3445	4026	4035
K_3	N/m	26,192	38,684	48,930	52,492
K_4	N/m	157,119	56,153	96,314	143,916
C_0	N s/m	107	153	164	170
C_1	N s/m	98	159	159	141
C_2	N s/m	39	25	29	35
C_3	N s/m	82	87	101	115
C_4	N s/m	128	75	100	125
f_0[a]	Hz	8.3	9.0	8.8	9.0
f_1[a]	Hz	25.9	36.4	37.3	34.3
f_2[a]	Hz	223.9	134.0	178.2	213.1
ξ_0		0.353	0.473	0.457	0.481
ξ_1		0.492	0.684	0.624	0.533
ξ_2		0.718	0.708	0.720	0.725

[a]Indicates that the frequencies are undamped natural frequencies.

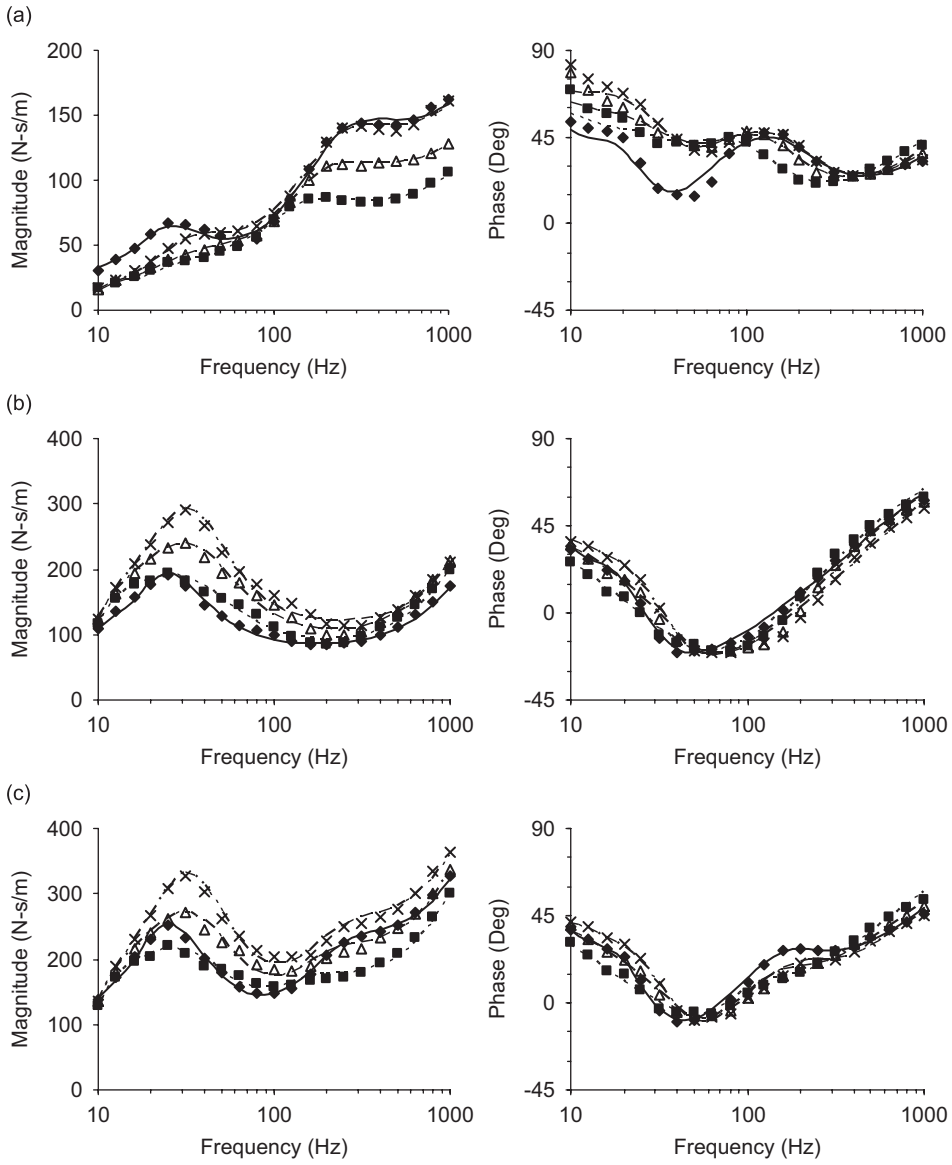

Fig. 3. Comparisons of experimental data and modeling results of the driving-point mechanical impedance of the hand–arm system measured: (a) finger magnitude and phase, (b) palm magnitude and phase, and (c) hand magnitude and phase. (♦, experiment 50 N grip-only; ————, model 50 N grip-only; ■, experiment 15 N grip and 35 N push; – – – – –, model 15 N grip and 35 N push; △, experiment 30 N grip and 45 N push; – · – · –, model 30 N grip and 45 N push; ×, experiment 50 N grip and 50 N push; —··—··—, model 50 N grip and 50 N push).

(M_1), listed in Table 1. This indicates that this resonance primarily depends on dynamic properties of these substructures. The second major resonance in the 100–300 Hz range relates to the fingers as it can be estimated from finger stiffness (k_4) and finger effective mass (M_2).

3.2. Examples of distributed vibration power absorption

As examples, Fig. 4 shows vibration spectra of three typical tools (a rock drill, a grinder with carborundum wheel, and a rammer) reported by Xu and Dings [27], and their corresponding vibration power absorption spectra calculated using the model for the combined action of 30 N grip and 45 N push. Table 2 lists the power

absorption values integrated from 10 to 1000 Hz using Eq. (13), and the ISO-weighted root-mean-square acceleration values integrated using Eq. (16). From the vibration spectra, it can be seen that the predominant vibration due to the rammer occurs in the low-frequency range (10–30 Hz). Its low-frequency components (<25 Hz) can be effectively transmitted to the arms, shoulder, neck, and head. The vibration power absorption is thus mostly distributed in these substructures, as clearly reflected in results shown in Fig. 4 and Table 2. On the other hand, the grinder vibration predominates at frequencies greater than 31.5 Hz and more than 82% of the total vibration power absorption is concentrated in the hand (in c_2, c_3 and c_4), as shown in Table 2. The rock drill is a tool that transmits vibration in both the low (20–31.5 Hz) and high (>100 Hz) frequency ranges. The resulting vibration power absorption thus occurs in both the fingers and the remaining hand–arm substructures.

Table 3 lists the results obtained from epidemiological study of these tools [27], together with the estimated 4-h equivalent energy absorption doses of the substructures. The results indicate that higher energy absorption corresponds to a larger prevalence of vibration-induced white finger for the three types of tools,

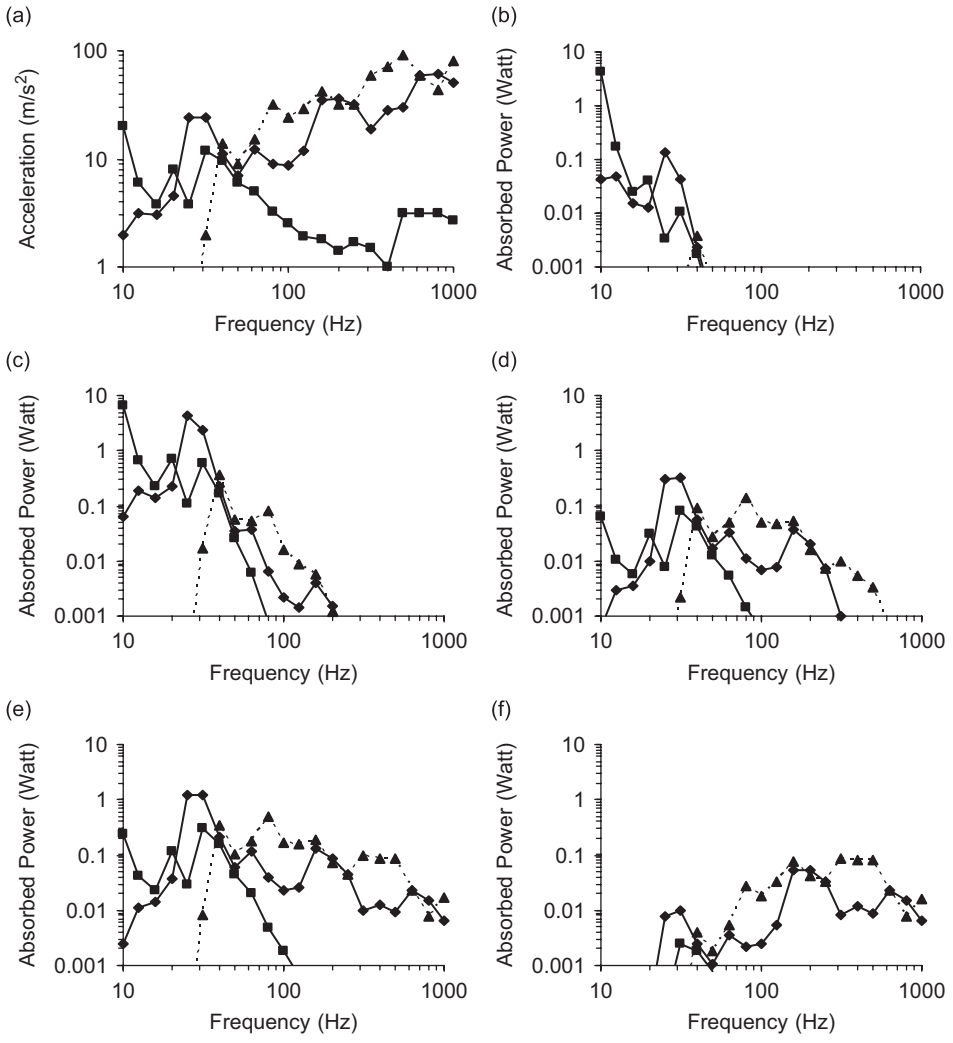

Fig. 4. Vibration spectra of three tools and their corresponding vibration power absorption distribution spectra predicted using the model for the combined action of 35 N grip and 45 N push: (a) tool vibration spectra; (b) power absorbed in c_0 or the shoulder, neck, and head; (c) power absorbed in c_1 or the forearm and upper arm; (d) power absorbed in c_2 or the hand back and the metacarpo-phalangeal joints and their surrounding tissues; (e) power absorbed in c_3 or the palm, wrist, and part of the forearm; and (f) power absorbed in c_4 or the fingers. (—■—, rammer; - - -▲- - -, grinder; and —◆—, rock drill).

Table 2
Comparisons of the ISO-weighted acceleration of three tools and the power absorption calculated using the tool spectra shown in Fig. 4 and the model for the combined action of 30 N grip and 45 N push

Tool category	Rock drill	Grinder with a carborundum wheel	Sand rammer
ISO-weighted acceleration (m/s^2)	22.44	13.62	22.62
Power absorption (W)			
Total	12.24	3.70	14.77
c_0: shoulder, neck, and head	0.30	0.01	4.60
c_1: forearm–upper arm–part of shoulder	7.57	0.60	8.92
c_2: hand back and metacarpo-phalangeal joints	0.84	0.50	0.26
c_3: palm–wrist–part of forearm	3.28	2.06	0.99
c_4: fingers	0.25	0.53	0.01

Table 3
Comparisons of the epidemiological results reported by Xu and Dings [27] and the 4-h equivalent acceleration and power absorptions

Tool category	Rock drill	Grinder with a carborundum wheel	Sand rammer
Work place reported in Ref. [27]	One lead and zinc mine, one gold mine, and two copper mines	Tool manufacturer	Aluminum factory
Number of examined workers reported in Ref. [27]	353	29	38
A_w: Calculated ISO-weighted acceleration (from Table 2) (m/s^2)	22.4	13.6	22.6
$A_w(4)$: 4-h equivalent acceleration reported in Ref. [27] (m/s^2)	16.3–26.7	10.3	6.4
T: Exposure duration (h)[a]	3.67	2.29	0.32
4 h equivalent vibration energy absorption (J)			
Total	161,791	30,474	17,024
c_0: shoulder, neck, and head	3935	43	5296
c_1: forearm–upper arm–part of shoulder	100,066	4950	10,278
c_2: hand back and metacarpo-phalangeal joints	11,102	4144	299
c_3: palm–wrist–part of forearm	43,409	16,960	1141
c_4: fingers	3276	4381	11
Prevalence of vibration-induced white finger reported in Ref. [27] (%)	50.5–62.5	82.7	13.2

[a]The exposure time is estimated from $T = 4[A_w(4)/A_w]^2$.

although the relationship is largely nonlinear. Such a relationship does not exist for any other measure presented in the table.

3.3. Frequency weightings

Fig. 5 shows the spectra of distributed vibration power absorptions estimated under a constant acceleration (10 m/s^2 root-mean-square) at each one-third octave band center frequency. At frequencies below 40 Hz, the power is mostly absorbed in the arms, shoulder and the upper body structures beyond the shoulder (c_0 and c_1). The power absorption in the palm, hand back, and wrist substructures (i.e., the sum powers dissipated in c_2 and c_3) suggests that vibration in the 16–50 Hz range would mostly affect the tissues in these substructures. The power absorbed in fingers (c_4) generally reveals two peak-like values: one in the hand–arm resonant frequency range and the other one in the finger resonant frequency range. The finger power absorption values

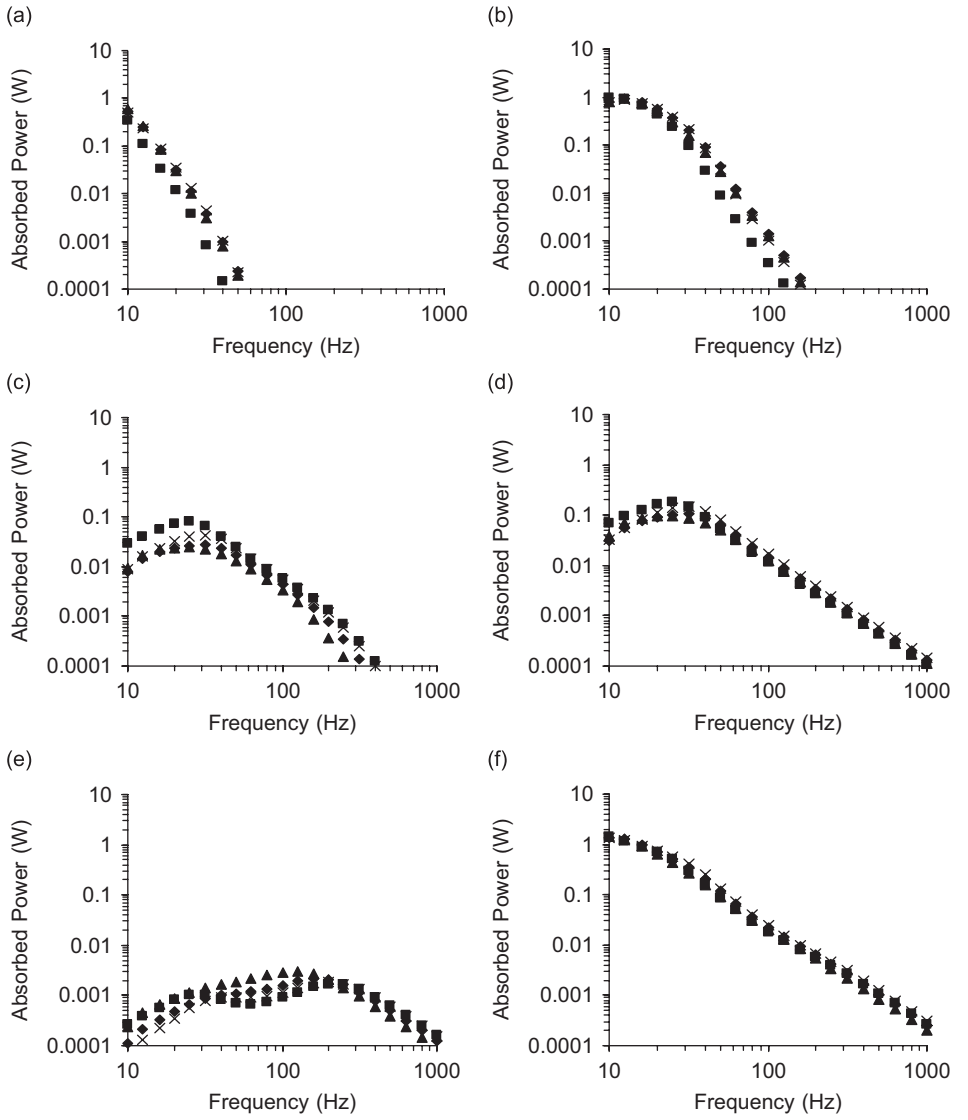

Fig. 5. Distribution of the vibration power absorption of the hand–arm system subjected to a constant acceleration vibration ($A = 10\,\mathrm{m/s^2}$ root-mean-square): (a) power absorbed in c_0 or the shoulder, neck, and head; (b) power absorbed in c_1 or the forearm and upper arm; (c) power absorbed in c_2 or the hand back and the metacarpo-phalangeal joints and their surrounding tissues; (d) power absorbed in c_3 or the palm and wrist; (e) power absorbed in c_4 or the fingers; and (f) total power absorbed in the entire hand–arm system (■, 50 N grip-only; ▲, 15 N grip and 30 N push; ◆, 30 N grip and 45 N push; ×, 50 N grip and 50 N push).

between the two resonant frequencies are also generally higher than those at frequencies less than 16 Hz and larger than 500 Hz.

Fig. 6 shows the frequency weightings derived from vibration power absorption, together with the ISO frequency weighting [3]. The vibration power absorption-based weightings for each substructure are normalized with respect to the maximum value of the vibration power absorption for the combined action of 30 N grip and 45 N push forces using Eq. (15). Consistent with results reported in Ref. [8], the weighting derived from total vibration power absorption is very similar to the ISO weighting. Although the ISO-weighting emphasizes the low-frequency components, the shoulder (c_0) vibration power absorption-based weighting emphasizes even lower frequency components. The wrist vibration power absorption-based weighting is also close to ISO-weighting but unlike the ISO it reveals relatively higher weighting up to 50 Hz. The finger weighting emphasizes the frequency range from 16 to 500 Hz.

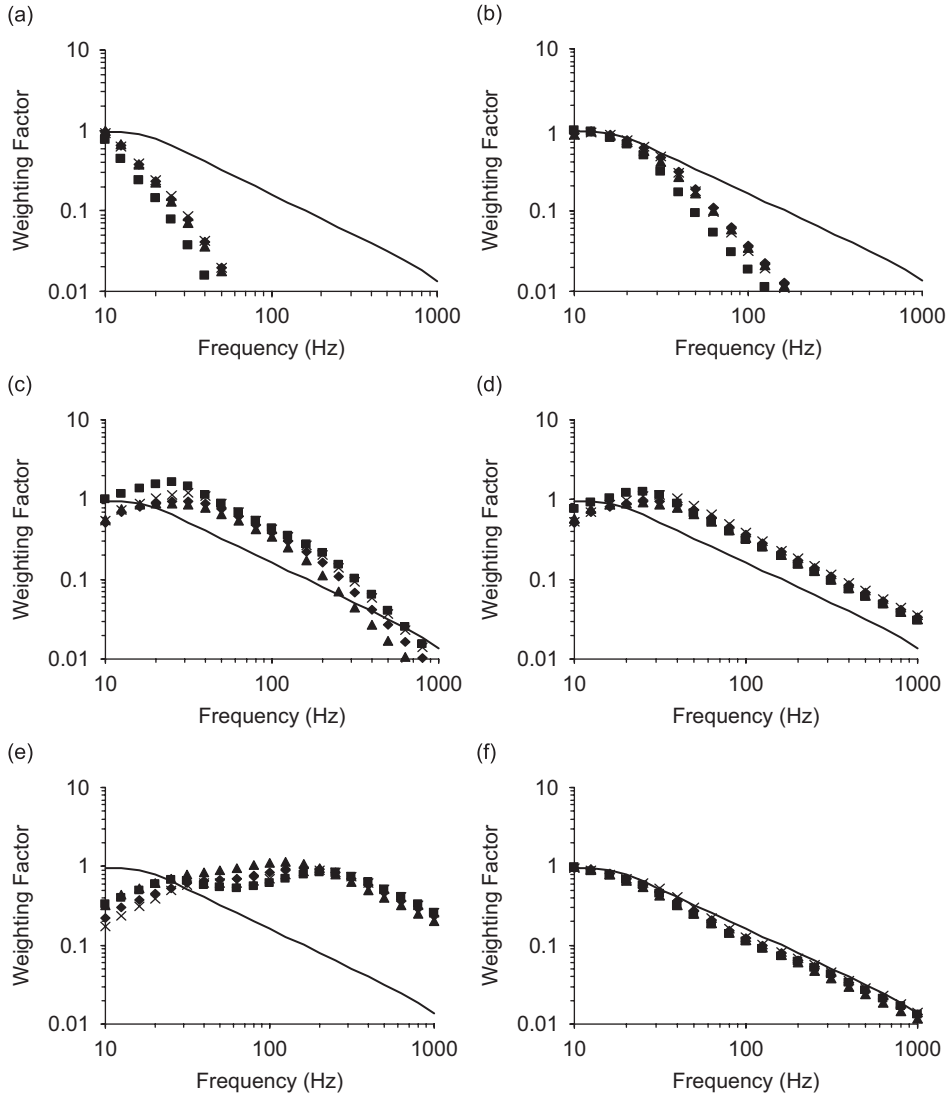

Fig. 6. Comparisons of the ISO frequency weighting and the vibration power absorption-based frequency weightings: (a) power absorbed in c_0 or the shoulder, neck, and head; (b) power absorbed in c_1 or the forearm and upper arm; (c) power absorbed in c_2 or the hand back and the metacarpo-phalangeal joints and their surrounding tissues; (d) power absorbed in c_3 or the palm and wrist; (e) power absorbed in c_4 or the fingers; and (f) total power absorbed in the entire hand–arm system (——, ISO frequency weighting; ■, 50 N grip-only; ▲, 15 N grip and 30 N push; ♦, 30 N grip and 45 N push; ×, 50 N grip and 50 N push).

3.4. Correlations among vibration measures

Table 4 lists coefficients of correlations among the vibration power absorption and acceleration measures. Fig. 7 shows several examples of the correlation relationships between the ISO-weighted root-mean-square acceleration and the distributed vibration power absorption. The results show trends that are consistent with those observed from the weighting curves shown in Fig. 6. The total vibration power absorption and vibration power absorption measured at the palm are highly correlated with the ISO-weighted acceleration. The vibration power absorptions distributed in the palm–wrist and arms also generally show good correlations with the ISO-weighted acceleration. The finger vibration power absorption, however, is poorly correlated with the ISO-weighted acceleration but it is highly correlated with the unweighted acceleration.

Table 4
Correlations among the vibration measures calculated using twenty tool spectra reported by Griffin [26]

Hand actions	15 N grip + 30 N push		30 N grip + 45 N push		50 N grip + 50 N push		50 N grip	
Vibration measures A_w: ISO-weighted acceleration A_u: unweighted acceleration	A_w	A_u	A_w	A_u	A_w	A_u	A_w	A_u
P_0: shoulder, neck, and head	0.7031	0.3064	0.7183	0.3384	0.7305	0.3621	0.6879	0.3145
P_1: forearm–upper arm–part of shoulder	0.9167	0.1074	0.9275	0.1308	0.9240	0.1265	0.8693	0.0307
P_2: hand back and metacarpo-phalangeal joints	0.9077	0.6602	0.8698	0.7222	0.8635	0.7173	0.9319	0.6149
P_3: palm–wrist–part of forearm	0.9054	0.7036	0.8760	0.7242	0.8713	0.7052	0.9367	0.5942
P_4: fingers	0.4287	0.9654	0.3925	0.9688	0.3819	0.9714	0.4210	0.9747
VPA into the palm	0.9818	0.3064	0.9898	0.3384	0.9925	0.3621	0.9847	0.3145
Total VPA	0.9918	0.3704	0.9966	0.3960	0.9977	0.4203	0.9930	0.3719

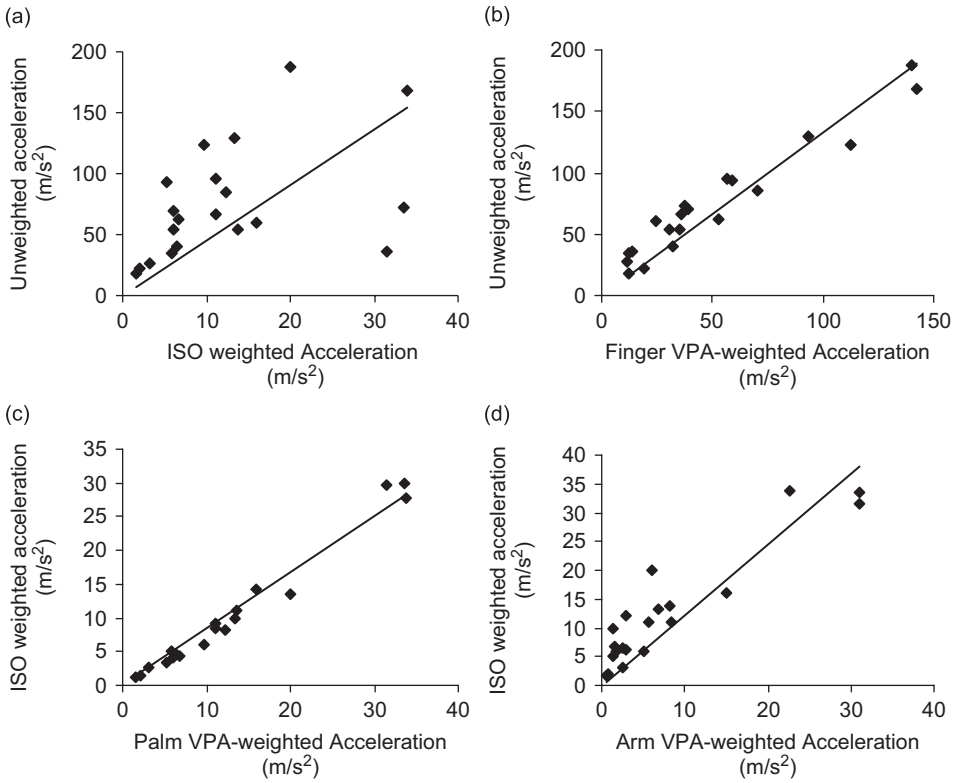

Fig. 7. Relationships among tool accelerations and vibration power absorption-weighted accelerations for 30 N grip + 45 N push: (a) unweighted acceleration vs ISO-weighted acceleration ($r = 0.4585$); (b) unweighted acceleration vs finger vibration power absorption-weighted acceleration ($r = 0.9688$); (c) ISO-weighted acceleration vs palm vibration power absorption-weighted acceleration ($r = 0.9898$); (d) ISO-weighted acceleration vs arm vibration power absorption-weighted acceleration ($r = 0.9275$) (♦, original data; ——, trend line).

4. Discussions

This study proposed a method for predicting vibration power absorption distributed in the major structures of the hand–arm system: fingers, back of the hand, palm–wrist–arm, and shoulder plus the structures beyond shoulder. Whereas no other experimental or modeling method has been developed to predict the vibration

power absorption distribution in these substructures, this method provides a tool to explore relationships between the substructure-specific power absorption and location-specific vibration-induced disorders. These relationships can be used to help determine how vibration causes hand–arm vibration syndrome and other vibration-induced upper limb disorders, and to develop better risk assessment methods for different structures of the upper limb system.

The results obtained in this study suggest that when the hand and fingers are subjected to a low-frequency vibration (<16 Hz), proportionally less vibration power is absorbed in these substructures. This is because the relative displacement between the fingers and contact surface of the tool is very small due to the high finger contact stiffness (Table 1), although the dynamic force at low frequencies (<16 Hz) could be the highest [28]. Thus, only a small portion of the energy is consumed in the finger contact area at low frequencies, and instead, vibration energy is largely transmitted up to the other parts of the hand–arm system and it is mainly absorbed in the arm, shoulder, and upper body. The transmission of energy into the upper limb may be responsible for the discomfort in the arms, shoulders, neck and head reported by operators of low-frequency tools such as sand rammers [29,30].

The vibration power absorption for the wrist, arm and shoulder primarily occurs in the 25–50 Hz frequency range (Fig. 5). This range encompasses the fundamental vibration frequencies of many percussive tools such as rock drills, chipping hammers and riveters [26,27]. The vibration power absorptions in the wrist–palm and arms are correlated with the ISO-weighted acceleration (Table 4). This may explain why the ISO-weighted acceleration yields a good correlation with wrist disorders [31]. Because the palm vibration power absorption is also correlated with the vibration power absorptions distributed in the palm–wrist–arm and shoulder (Table 4) and it can be directly measured in the field using a palm adapter equipped with an accelerometer and a force sensor (see, for example, Ref. [32]), the palm vibration power absorption may be used to represent the location-specific vibration power absorptions for specifically assessing the risk of developing vibration-induced disorders and discomfort in the wrist, arms, and shoulder.

The most recognized disorder associated with exposure to hand-transmitted vibration is vibration-induced white finger. In Table 3, the prevalence of vibration-induced white finger in rammer operators working in an aluminum factory was 13.2%, and the ISO-weighted acceleration was 22.6 m/s^2 [27]. However, according to the data reported by Xu et al. [27] and Tominaga [30], the average prevalence of vibration-induced white finger among rammer operators was 0.0% and 2.2%, and the corresponding ISO-weighted accelerations were 30.0 and 39.9 m/s^2, respectively. Therefore, the data listed in Table 3 may represent the worst case of vibration-induced white finger prevalence among rammer workers. According to the data summarized by Griffin [16], the prevalence of vibration-induced white finger in grinders in the aluminum factor may also represent the worst case. The data in Table 3 [27], along with data from other studies [30,33–38] do not support the use of ISO-weighted acceleration for predicting vibration-induced white finger risk. On the other hand, the data listed in Table 3 show a positive relationship between the finger vibration power absorption and vibration-induced white finger, suggesting that the finger vibration power absorption is a better method for assessing the risk of developing vibration-induced white finger.

The two major resonances of the hand–arm system may also contribute to the development of finger disorders. According to the data summarized by Griffin [13], the prevalence of vibration-induced white finger is highest with the use of tools that have a predominant vibration frequency in the 25–500 Hz range. The majority of these tools have dominant vibration frequencies that fall in the range of 25–50 Hz or 100–300 Hz. These frequency ranges are in the ranges of the two major resonant frequency ranges of the hand–arm system (16–50 Hz and 100–300 Hz). Thus, the higher prevalence of vibration-induced white finger in workers using tools with these dominant frequencies could be attributed to the higher magnitudes of hand-transmitted vibration and to the presence of hand–arm system resonances, which could result in higher tissue strain and stress in the fingers. Coincidently, the finger vibration power absorption-based weighting is also high from 16 to 500 Hz. Thus, the responses of the fingers to these frequencies (16–500 Hz) and the resonance effects are reasonably reflected in the finger vibration power absorption-based frequency weighting.

Griffin et al. [38] reported that unweighted acceleration due to hand-transmitted vibration exposure provided a better correlation with vibration-induced white finger than the ISO-weighted acceleration. Table 4 and Fig. 7 show that vibration power absorption also is highly correlated with the unweighted acceleration.

These observations further suggest that the finger vibration power absorption may have an association with the vibration-induced white finger. Because the unweighted acceleration is only a measure of vibration hazard on the tool, the finger vibration power absorption is theoretically a better measure as it takes into account both the tool vibration and the finger biodynamic response. It is thus anticipated that the finger vibration power absorption may provide a better prediction of risk of vibration-induced finger disorders than either of the acceleration methods.

Reduction in peripheral sensation is also a common symptom of hand–arm vibration syndrome, which can be detected by measuring the fingertip vibrotactile threshold. The acute effect of the vibration exposure on the peripheral sensation is frequently evaluated by measuring the temporal threshold shift after exposure to vibration at a certain frequency (see, for example Refs. [39,40]). Fig. 8 shows a typical group of temporal threshold shift data reported by Harada and Griffin [39]. The temporal threshold shift values shown in this figure were greatest in subjects exposed to vibration between 100 and 300 Hz. The finger vibration power absorption also is high in this frequency range (Fig. 5e). Thus, the finger vibration power absorption may play a role in the threshold shift. This suggests that the finger vibration power absorption method may not only be potentially useful for assessing vibration-induced risk of vibration-induced white finger, but it may also be used to help assess the risk of developing sensory dysfunction in the fingers.

It is should be noted that the 5-degree-of-freedom lumped parameter model does not accurately represent the continuous fingers–hand–arm system and thus may not predict the location-specific responses precisely. This modeling approach, however, offers a simple means to enhance an understanding of the fundamental characteristics of vibration energy distribution, and relationships between the vibration power absorption distribution and the location-specific vibration-induced injuries and disorders. Since the model parameters are identified on the basis of experimental data acquired at the hand–handle contact points, the model parameters and vibration power absorption distribution in the substructures closer to the contact points may be more reliable than of those farther away from the contact points. Moreover, many factors could affect the power absorption. For example, the arm posture could greatly affect the low-frequency vibration transmission [41] thus the power absorption in arms and the upper body. The biodynamic response to z_h-axis vibration considered in this study is also generally different from those under vibration along other directions [42]. Since the tools may have different dominant vibration axes, it would be inaccurate to use the z_h-axis vibration power absorption alone to represent the distributed vibration power absorptions for the types of tools of concern in this study. Moreover, the validity of the hand-force-specific linear model may be questionable under large magnitudes of vibration, particular in the first resonant frequency range (16–50 Hz) and at lower frequencies. Such vibration may cause large magnitudes of relative hand–handle displacements and lead to possible intermittent loss of hand contact with the tool handle. The linear models could thus yield an overestimate of vibration power absorption under high intensity vibration. This suggests that the estimated vibration power absorptions for some tools such as rock drill, road breaker, and rammer could be overestimated. The possible

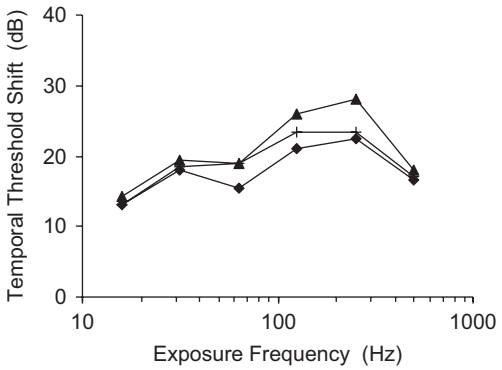

Fig. 8. Comparison of the finger vibration power absorption-based frequency weighting and those derived from vibrotactile temporal threshold shift after exposure to vibration reported by Harada and Griffin [39] (—+—, threshold measured at 125 Hz; —▲—, threshold measured at 250 Hz; and —◆—, threshold measured at 500 Hz).

overestimation may also because the power absorption may not increase linearly with the impedance and the squared acceleration or the impedance could change with the vibration magnitude. All the above-mentioned factors, however, may not change the observed basic trends in vibration power absorption distributions identified in this study. This is because the transmission of vibration from a tool is governed by the general rule: low-frequency vibration can transmit farther from the hand–handle interface than higher frequency vibration [43,44]. Despite all the limitations, the proposed biodynamic approach for quantifying the distributed vibration power absorptions offers some potential for health risk assessments of hand-transmitted vibration. The proposed local energy method can be further enhanced when more experimental data and knowledge of the influencing factors are available.

5. Conclusions

A method for predicting the absorbed power distributed in various substructures of the hand–arm system exposed to vibration is proposed. A five-degrees-of-freedom model of the hand–arm system with finger- and palm-side driving points is used to estimate the absorbed power distributed in fingers, hand back, palm–wrist, arms, and shoulder and structures beyond the shoulder. The vibration power absorption was found to be mostly distributed in the arm and shoulder when operating low-frequency tools, such as rammers. The power absorption was mostly concentrated in the fingers and hand when operating high-frequency tools, such as grinders. The major resonances of the hand–arm system were closely reflected in vibration power absorption distributed in the fingers. The vibration power absorptions further suggested that vibration exposure in the frequency range of 16–500 Hz would generally pose a higher risk of developing fingers disorders than exposure to vibration at other frequencies. Whereas the finger vibration power absorption was found to be correlated with unweighted acceleration measured on many tools, the vibration power absorption distributed in the palm–wrist–arm system was correlated with the ISO-weighted acceleration. These could provide better understanding of some of the findings of the reported physiological and epidemiological studies. Although further studies are vital to take into account the contributions due to major influencing factors and to improve the hand–arm system models, the proposed local energy method showed a promising potential for assessment of exposure dosage and associated health effects.

Disclaimers

The content of this publication does not necessarily reflect the views or policies of the National Institute for Occupational Safety and Health (NIOSH), nor does mention of trade names, commercial products, or organizations imply endorsement by the US Government.

References

[1] NIOSH 1997. Musculoskeletal disorders and workplace factors—a critical review of epidemiologic evidence for work-related musculoskeletal disorders of the neck, upper extremity, and low back, *DHHS (NIOSH) Publication No. 97-141*, Cincinnati, OH, USA.

[2] G. Gemne, W. Taylor, Foreword: hand–arm vibration and the central autonomic nervous system, *Journal of Low Frequency Noise and Vibration (Special Volume)* (1983) 1–12.

[3] ISO 5349-1, Mechanical Vibration—Measurement and Evaluation of Human Exposure to Hand-transmitted Vibration—part 1: General Guidelines. International Organization of Standard, Geneva, Switzerland, 2001.

[4] M. Bovenzi, Exposure–response relationship in the hand–arm vibration syndrome: an overview of current epidemiology research, *International Archives of Occupational and Environmental Health* 71 (1998) 509–519.

[5] M.J. Griffin, Foundations of hand-transmitted vibration standards, *Nagoya Journal of Medical Science* 57 (1994) 147–164.

[6] R.G. Dong, J.Z. Wu, D.E. Welcome, Recent advances in biodynamics of hand–arm system, *Industrial Health* 43 (2005) 449–471.

[7] J.Z. Wu, K. Krajnak, D.E. Welcome, R.G. Dong, Analysis of the dynamic strains in a fingertip exposed to vibration: correlation to the mechanical stimuli on mechanoreceptors, *Journal of Biomechanics* 39 (2006) 2445–2456.

[8] R.G. Dong, D.E. Welcome, T.W. McDowell, J.Z. Wu, A.W. Schopper, Frequency weighting derived from power absorption of fingers–hand–arm system under z_h-axis, *Journal of Biomechanics* 39 (2006) 2311–2324.

[9] L. Burström, Absorption of Vibration Energy in the Human Hand and Arm, Doctorial Thesis, Lulea University of Technology, Sweden, 1990.
[10] Y. Aldien, D.W. Welcome, S. Rakheja, R.G. Dong, P.-E. Boileau, Contact pressure distribution at hand–handle interface: role of hand forces and handle size, *International Journal of Industrial Ergonomics* 35 (2005) 267–286.
[11] I.M. Lidström, Vibration injury in rock drillers, chiselers, and grinders: some views on the relationship between the quantity of energy absorbed and the risk of occurrence of vibration injury, *Proceedings of the International Conference on Hand– Arm Vibration*, Cincinnati, USA, 1977, pp. 77–83.
[12] L. Burström, R. Lundström, Mechanical energy absorption in human hand–arm exposed to sinusoidal vibration, *International Archives of Occupational and Environmental Health* 61 (1988) 213–216.
[13] R.G. Dong, A.W. Schopper, T.W. McDowell, D.E. Welcome, J.Z. Wu, W.P. Smutz, C. Warren, S. Rakheja, Vibration energy absorption (VEA) in human fingers–hand–arm system, *Medical Engineering and Physics* 26 (2004) 483–492.
[14] T. Miwa, Evaluation methods for vibration effect—part 6: measurements of unpleasant and tolerance limit levels for sinusoidal vibrations, *Industrial Health* 6 (1968) 18–27.
[15] T. Miwa, Evaluation methods for vibration effects—part 4: measurement of vibration greatness for whole-body and hand in vertical and horizontal vibration, *Industrial Health* 6 (1968) 1–10.
[16] M.J. Griffin, *Handbook of Human Vibration*, Academic Press, London, UK, 1990.
[17] J.Z. Wu, D.E. Welcome, R.G. Dong, Three-dimensional finite element simulations of the mechanical response of the fingertip to static and dynamic compressions, *Computer Methods in Biomechanics and Biomedical Engineering* 9 (2006) 55–63.
[18] R.G. Dong, J.H. Dong, J.Z. Wu, S. Rakheja, Modeling of biodynamic responses distributed at the fingers and the palm of the human hand–arm system, *Journal of Biomechanics* 40 (2007) 2335–2340.
[19] R.G. Dong, S. Rakheja, A.W. Schopper, B. Han, W.P. Smutz, Hand-transmitted vibration and biodynamic response of the human hand–arm: a critical review, *Critical Reviews in Biomedical Engineering* 29 (2001) 391–441.
[20] S. Rakheja, J.Z. Wu, R.G. Dong, A.W. Schopper, A comparison of biodynamic models of the human hand–arm system for applications to hand-held power tools, *Journal of Sound and Vibration* 249 (2001) 55–82.
[21] S. Kihlberg, Biodynamic response of the hand–arm system to vibration from an impact hammer and a grinder, *International Journal of Industrial Ergonomics* 16 (1995) 1–8.
[22] R.G. Dong, D.E. Welcome, T.W. McDowell, J.Z. Wu, Biodynamic response of human fingers in a power grip subjected to a random vibration, *Journal of Biomechanical Engineering* 126 (2004) 447–457.
[23] R.G. Dong, T.W. McDowell, D.E. Welcome, Biodynamic response at the palm of the human hand subjected to a random vibration, *Industrial Health* 43 (2005) 241–253.
[24] D.B. Chaffin, G.B. Andersson, B.J. Martin, *Occupational Biomechanics*, Wiley, New York, 1999.
[25] W. Karwowski, W.S. Marras, *Occupational Ergonomics*, CRC Press, New York, USA, 1999.
[26] M.J. Griffin, Measurement, evaluation, and assessment of occupational exposures to hand-transmitted vibration, *Occupational and Environmental Medicine* 54 (1997) 73–89.
[27] Z. Xu, H.C. Ding, M.P. Ding, A study of dose–effect relationships for vibration induced white finger, *Proceedings of the Fifth International Conference on Hand– Arm Vibration,* Kanazawa, Japan, 1990, pp. 305–308.
[28] R.G. Dong, D.E. Welcome, J.Z. Wu, Estimation of the biodynamic force acting at the interface between hand and vibrating surface, *Industrial Health* 43 (2005) 516–526.
[29] Personal conversations with workers in a steel foundry, 2001.
[30] Y. Tominaga, The relationship between vibration exposure and symptoms of vibration syndrome, *Journal of Science of Labour* (1993) 1–14.
[31] J. Malchaire, A. Piette, N. Cock, Associations between hand–wrist musculoskeletal and sensorineural complaints and biomechanical and vibration work constraints, *Annals of Occupational Hygiene* 45 (2001) 479–491.
[32] L. Burström, R. Lundström, Portable equipment for field measurement of the hand's absorption of vibration energy, *Safety Science* 28 (1998) 15–20.
[33] M. Bovenzi, A. Franzinelli, F. Strambi, Prevalence of vibration-induced white finger and assessment of vibration exposure among travertine workers in Italy, *International Archives of Occupational and Environmental Health* 61 (1988) 25–34.
[34] J. Starck, P. Jussi, P. Ilmari, Physical characteristics of vibration in relation to vibration-induced white finger, *American Industrial Hygiene Association Journal* 51 (1990) 179–184.
[35] T. Nilsson, L. Burström, M. Hagberg, Risk assessment of vibration exposure and white fingers among platers, *International Archives of Occupational and Environmental Health* 61 (1989) 473–481.
[36] R. Dandanell, K. Engstrom, Vibration from riveting tools in the frequency range 6 Hz–10 MHz and Raynaud's phenomenon, *Scandinavian Journal of Work, Environment & Health* 12 (1986) 338–342.
[37] Y. Tominaga, New frequency weighting of hand–arm vibration, *Industrial Health* 43 (2005) 509–515.
[38] M. Griffin, M. Bovenzi, C.M. Nelson, Dose–response patterns for vibration-induced white finger, *Occupational and Environmental Medicine* 60 (2003) 16–26.
[39] N. Harada, M.J. Griffin, Factors influencing vibration sense thresholds used to assess occupational exposure to hand-transmitted vibration, *British Journal of Industrial Medicine* 48 (1991) 185–192.
[40] S. Maeda, M.J. Griffin, Temporary threshold shifts in fingertip vibratory sensation from hand-transmitted vibration and repetitive shock, *British Journal of Industrial Medicine* 50 (1993) 360–367.
[41] H. Sakakibara, T. Kondo, M. Miyao, S. Yamada, T. Nakagawa, F. Kobayahsi, Y. Ono, Transmission of hand–arm vibration to the head, *Scandinavian Journal of Work, Environment & Health* (1986) 359–361.

[42] ISO-10068, *Mechanical Vibration and Shock—Free, Mechanical Impedance of the Human Hand– Arm System at the Driving Point*, International Organization of Standard, Geneva, Switzerland, 1998.
[43] I. Pyykkö, M. Färkkilä, J. Toivanen, O. Korhonen, J. Hyvarinen, Transmission of vibration in the hand–arm system with special reference to changes in compression force and acceleration, *Scandinavian Journal of Work, Environment & Health* 2 (1976) 87–95.
[44] D. Reynolds, E.N. Angevine, Hand–arm vibration, part II: vibration transmission characteristics of the hand and arm, *Journal of Sound Vibration* 51 (1977) 255–265.